

Supplementary Information

A Instrumental Water Cross-Sensitivity Correction

Previous studies have found a cross-sensitivity of reported mixing ratios of gases to atmospheric water vapour with the OA-ICOS in two separate ways; through dilution and pressure broadening effects (Chen et al., 2010; Hiller et al., 2012). The effect of H₂O on the gas mixing ratios that is specific to each instrument and was determined by changing humidity added to the gas standard stepwise from 0 – 26,000 ppm of H₂O. Multiple stepwise H₂O tests were run on the instrument, where the average of the values at each step of H₂O was used to calculate a correction factor shown in Equation 1.

$$[\text{CH}_4]_{dry} = [\text{CH}_4]_{CP} + (1.4667 \times 10^{-11} \times [\text{H}_2\text{O}]_{CP}^2) + (2.0233 \times 10^{-6} \times [\text{H}_2\text{O}]_{CP}) - 6.3502 \times 10^{-5} \quad [1]$$

One example of these tests is shown in Figure S1, where the difference between the uncorrected wet (light gray) and dry mole fraction (dark gray) is attributed to dilution effects because the wet mole fraction is calculated by the number of moles of the atmospheric species is divided by the number of moles in wet air. The remaining difference between the uncorrected and corrected dry mole fraction (green) is attributed to pressure broadening effects, where the corrected mixing ratio was calculated from Equation 1. In total, there was a ~3% discrepancy between the wet mixing ratio and corrected dry mixing ratio at 26,000 ppm H₂O.

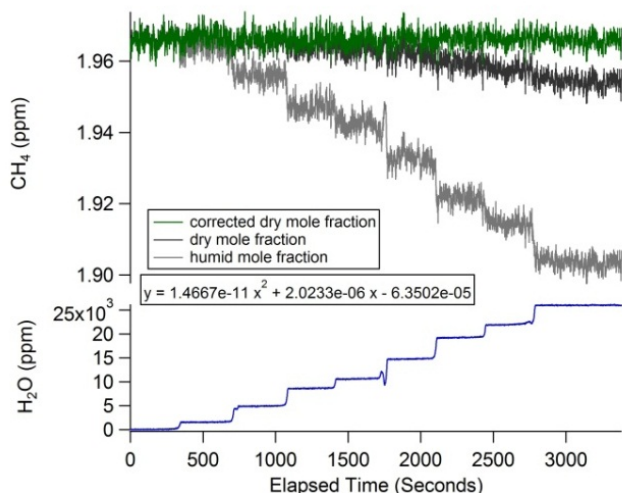


Figure S1: One stepwise test of CH₄ where moisture was added over 8 different levels from 0 – 26,000 ppm with the uncorrected (gray) and corrected (green) mixing ratios.

The instrument was also tested for its accuracy in measuring water using a dewpoint generator (model LI-610, LI-COR Inc., Lincoln, Nebraska) which was attached to the inlet line similarly to the calibration gas tests. The measured H₂O mixing ratio was plotted against the set

dew point temperature converted into ppm of H₂O in Figure S2. The FGGA underestimated the mixing ratio of H₂O as relative humidity was increased, although there was still a linear correlation ($R^2 = 0.9994$). As the accuracy of the dew point generator could not be properly determined, the accuracy of the FGGA was simply judged by the relative values shown in Figure S2 and the underestimation of H₂O was not corrected for within the FGGA. The absolute value of the H₂O mixing ratio was not important in the calculation of the fluxes, although the relative mixing ratio of H₂O to CO₂ and CH₄ was used to correct for dilution and pressure broadening effects.

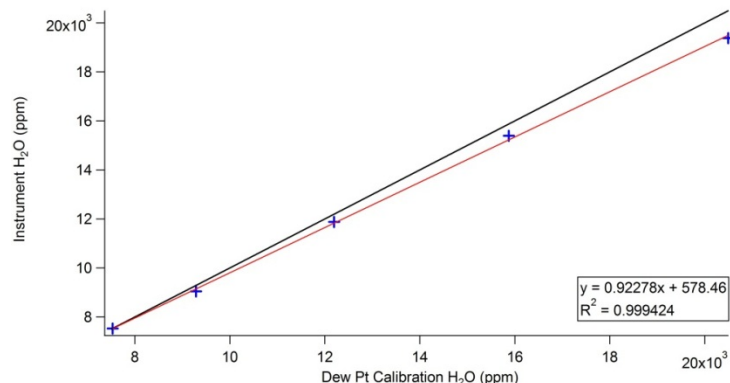


Figure S2: Calibration of water measurements using a Dew Point Generator.

B Instrument Accuracy and Precision

The instrument was tested for its stability, accuracy, and precision before being deployed at the field site, during the field campaign, and after being brought back to the laboratory. A calibration gas (Linde Canada Ltd., Brampton, Ontario) certified at $2010 \pm 100 \text{ nmol mol}^{-1}$ for CH₄ was used to test the accuracy of the instrument. An example of one audit run over 25 minutes is shown in Figure S3 where the instrument reported an average mixing ratio with the standard deviation of $1999 \pm 2 \text{ nmol mol}^{-1}$. Before the instrument was brought to the field, 20 audits were conducted over a period of three months with a range in mixing ratios between 1990 – 2004 nmol mol^{-1} . When the instrument was brought back from the field, three audits were run on the instrument with mixing ratios ranging between 1998 – 2000 nmol mol^{-1} showing good agreement with audits run before the field campaign.

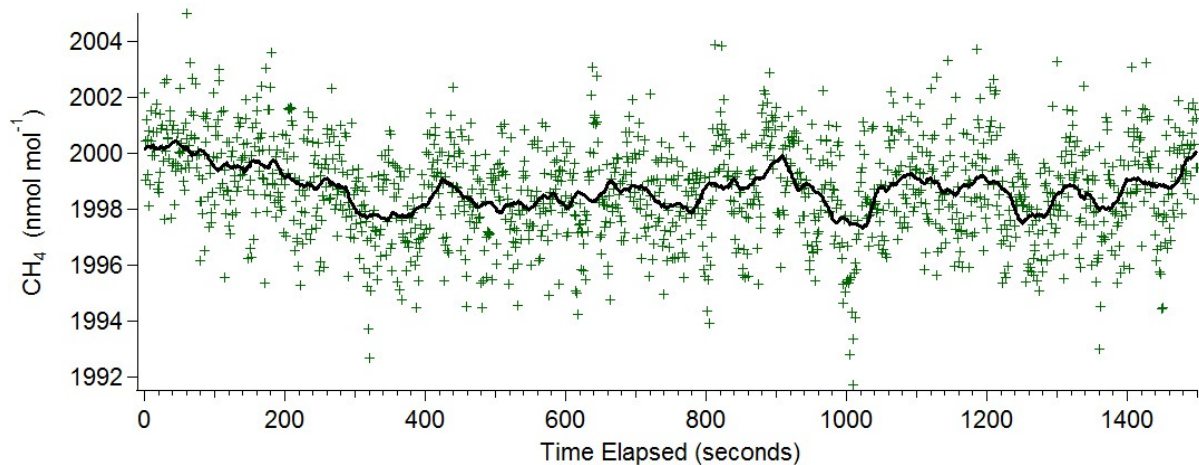


Figure S3: Time series of one audit at 1 Hz using low flow setting after the instrument was brought back from the field.

C High Frequency Noise Correction

Although fluxes are typically less influenced than mixing ratios by random noise, which should not correlate strongly with vertical wind variations (Smeets et al., 2009), instrumental noise can still modify the high frequency region of the cospectrum if the noise level is high enough. Instrumental noise was observed to influence the high frequency part of the cospectrum as a result of the high pumping speed shown in Figure . The noise influenced CH_4 more than the CO_2 gas channel, presumably due to a lower signal-to-noise ratio. From the average of 74 cospectra daytime ensembles of CH_4 and vertical wind, a conservative estimate of the frequency threshold beyond which noise dominate the covariance was determined to be 0.2 Hz. To correct for this, cospectral similarity of the scalars was assumed where the percent relative contribution to the fluxes within the same frequency range of other scalars such as sonic temperature and open path (OP) CO_2 was used as a reference and applied to the cospectrum of the closed path (CP) CH_4 and CO_2 from the FGGA on a half-hour basis.

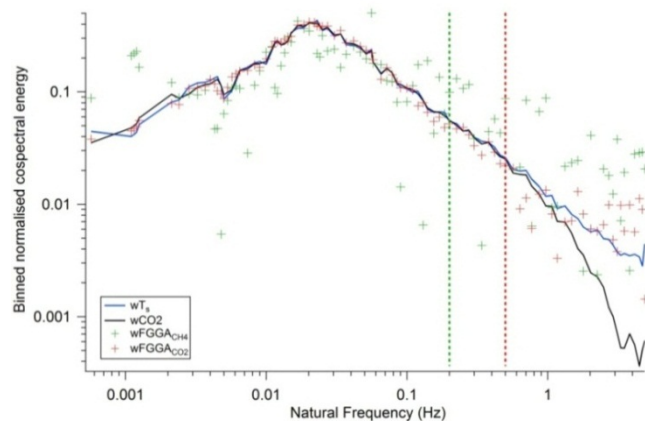


Figure S4: Averaged smoothed normalized cospectra from 74 daytime ensembles of sonic temperature, OP CO₂, and CP CO₂ and CH₄ plotted as a function of natural frequency with an average stability and wind speed range of $z/L=-0.074$ and $\bar{u}=2.7\pm 0.5$ m s⁻¹.

The contribution of noise to the cospectrum above 0.2 Hz was also used to determine the flux limit of detection as a result of noise from the instrument Figure . In theory, if a constant mixing ratio is measured for 30 minutes at 10 Hz, the combination of this data with any arbitrary 30 minutes of vertical wind data from the sonic anemometer should result in a flux of zero. Data were obtained from calibration runs that used calibration gas mixed with zero-air on the instrument over 30 minutes at high frequency and processed with vertical wind data from the entire measurement period to determine the limit of detection of the fluxes. The limit of detection for CH₄ fluxes was calculated at ± 5.3 nmol m⁻² s⁻¹. Any values within this range were considered indistinguishable from zero, although were still used during the interpretation of data. There was also no observable diurnal trend in the covariance of the noise cospectrum with vertical wind.

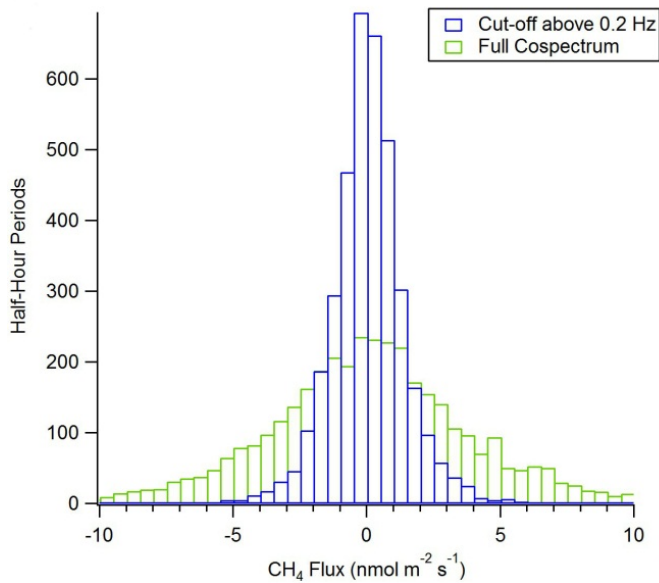


Figure S5: Histogram of the covariance the entire cospectrum (green) and the contribution above the frequency cut-off of 0.2 Hz (blue) for CH₄ calculated from a constant mixing ratio from the calibration gas from each half-hour period.